Residual Structure in Large Fragments of Staphylococcal Nuclease: Effects of Amino Acid Substitutions†

David Shortle* and Alan K. Meeker

Department of Biological Chemistry, The Johns Hopkins University School of Medicine, Baltimore, Maryland 21205

Received July 26, 1988; Revised Manuscript Received August 31, 1988

ABSTRACT: In an attempt to develop a model of the denatured state of staphylococcal nuclease that can be analyzed experimentally under physiological conditions, a series of four large fragments of this small protein which extend from residues 1 to 103, 1 to 112, 1 to 128, and 1 to 136 have been generated through the overexpression of nuclease genes containing stop codons at defined positions. Large amounts of protein fragments were accumulated in induced cells and were purified by carrying out all fractionation steps in the presence of 6 M urea. The far-ultraviolet circular dichroism spectra of all four fragments suggested the presence of small to moderate amounts of residual structure. When the CD spectra were monitored as a function of concentrations of the tight-binding ligands Ca^{2+} and thymidine 3′,5′-bisphosphate and the known affinity constants for wild-type nuclease (1–149) were used, apparent equilibrium constants of 160 and 2000 for the reversible denaturation reaction for fragments 1–136 and 1–128, respectively, were estimated. Four single and two double mutations, all of which exhibit unusual behavior in the full-length protein on solvent denaturation [Shortle, D., & Meeker, A. K. (1986) *Proteins: Struct., Funct., Genet. 1*, 81–89] and thermal denaturation [Shortle, D., Meeker, A. K., & Freire, E. (1988) *Biochemistry 27*, 4761–4768], were recombined into the 1–136 and 1–128 fragment expression vectors, and purified mutant fragments were characterized. The CD spectra of the class I mutants (V66L, G88V, and V66L+G88V) showed evidence of an increase in residual structure relative to the wild-type fragment, whereas the spectra of the class II mutants (A69T, A90S, and A69T+A90S) showed evidence of a decrease in residual structure. Analysis of the apparent hydrodynamic radii of these fragments by high-performance gel filtration provided independent support for large changes in residual structure on addition of these amino acid substitutions. When the ellipticity at 222 nm and the elution volume were monitored as a function of guanidine hydrochloride concentration, fragment 1–128 containing class I mutations exhibited a sigmoidal transition suggestive of a cooperative breakdown in the residual structure. From these observations, the existence of two alternative denatured states of staphylococcal nuclease is inferred: D1 representing a compact, structured, but nonnative state, and D2 representing an expanded, less structured state. The behavior of the two classes of mutations on reversible denaturation can be explained as resulting from a relative stabilization of the D1 state (class I) or a relative stabilization of the D2 state (class II).

The native state of many proteins can be demonstrated to exist in a dynamic equilibrium with an alternative, less structured state known as the denatured state. The equilibrium constant K_d for this reversible reaction is determined by the free energy difference ΔG_d between these two states. For almost all of the proteins that have been studied, ΔG_d, under physiological conditions of temperature, pH, and salt concentration, falls in the range of 5–15 kcal/mol (Pace, 1975). Consequently, the fraction of protein molecules in the denatured state under such conditions is vanishingly small—between 10^{-3} and 10^{-10}.

Obviously, attempts to characterize the physical properties of the denatured state of a protein are complicated by its very low abundance under physiological conditions. The denatured state can be stabilized readily by changing the conditions of solution—elevated temperatures, extremes of pH, and addition of denaturants. However, there is reason to question whether the denatured state obtained through these types of perturbation has the same structure as the denatured state under physiological conditions (Tanford, 1969). Both experimental observations (Aune et al., 1967; Tsong, 1974) and basic principles from the physical chemistry of polymers (Flory, 1953; Lumry et al., 1966; Dill, 1985) suggest that the denatured state is likely to change significantly as the conditions of solution are changed.

In the course of characterizing the effects of a number of different amino acid substitutions on the reversible denaturation reaction of staphylococcal nuclease, we have concluded that some of these sequence changes must be altering the structure present in the denatured state. Initially, we observed striking variations in the rate of change of the apparent ΔG_d with respect to changes in the concentration of either Gdn·HCl or urea ($d\Delta G/dC_{den}$) (Shortle & Meeker, 1986). The amino acid substitutions that increased $d\Delta G/dC_{den}$ could only be explained within the current understanding of the mechanism of action of these denaturants by proposing that they increase the solvent-accessible surface area of the denatured state. Likewise, substitutions that decreased the value of $d\Delta G/dC_{den}$ could most simply be explained by decreases in the solvent-accessible surface area of the denatured state. On further characterization of this same set of mutant nucleases, we observed changes in the apparent ΔC_p for reversible thermal denaturation (Shortle et al., 1988). Again, within the context of the current theories of the physical–chemical basis for ΔC_p, the proposal was made that amino acid substitutions which increased ΔC_p do so by causing the exposure of more hydro-

† This work was supported by a grant (GM34171) from the National Institutes of Health.

* Correspondence should be addressed to this author.

0006-2960/89/0428-0936$01.50/0

phobic surface in the denatured state and substitutions which decreased ΔC_p have the opposite effect of reducing exposure of hydrophobic surface.

In this report we describe a different approach to stabilizing the denatured state to permit its characterization by physical methods. Instead of changing the conditions of solution, we have altered the chemical structure of the polypeptide chain by removing a small number of amino acid residues from the carboxy-terminal end. Characterization of these large fragments of staphylococcal nuclease suggests that they may be reasonable models of the denatured state under physiological conditions. In addition, the effects of the two types of amino acid substitutions on the residual structure present in these large fragments were examined in order to test the conclusion that they induce significant changes in the structure of the denatured state.

Experimental Procedures

Recombinant DNA. Wild-type staphylococcal nuclease (1–149) and all nuclease fragments were produced by induction of plasmid pL9, a λ pL promoter plasmid derived from pNJS (Hibler et al., 1987). In the construction of pL9, the high-copy origin of pUC19 was substituted into pNJS, and the six extraneous codons between the initiator ATG and codon 1 of mature nuclease were deleted by using a synthetic oligonucleotide. Ocher mutations (TAA) at positions 113, 129, and 137 were isolated from a collection of randomly induced mutations (Shortle & Lin, 1985). After placing these mutations into pL9, sequences between codons 27 and 101 were deleted and a unique *Xho*I site was inserted in their place to permit heteroduplex recombination (Shortle & Lin, 1985) of the V66L, G88V, V66L+G88V, A69T, A90S, and A69T+A90S mutations (Shortle & Meeker, 1986) into pL9 derivatives containing the different stop codons. A stop codon at position 104 was constructed by ligating the octanucleotide CTCTAGAG onto linears of pL9 generated by *Hin*dIII cleavage and filling in the 5′ overhanging end with Klenow fragment polymerase.

Protein Purification. Escherichia coli strain AR120 (Mott et al., 1985) carrying the appropriate recombinant plasmid and grown to a density of 5×10^8/mL at 37 °C in LB broth was induced for protein production by adding nalidixic acid to a final concentration of 40 mg/L. After an additional 4 h of growth, the cell pellet was collected by centrifugation and then resuspended in one-tenth volume of the original culture of 6 M urea/50 mM Tris·HCl,[1] pH 9.2/1 mM EDTA/0.2 M NaCl. After this suspension was shaken gently on ice for 30 min, followed by centrifugation, the supernatant was recovered. To this volume of extract was added an equal volume of ice-cold ethanol, and precipitation was promoted for 1 h at −20 °C. The precipitate was discarded after centrifugation, and an additional 2 volumes of ethanol was added to the supernatant. After incubation of this solution at −20 °C for 1–2 h, the precipitate was recovered by centrifugation, dried briefly by lyophilization, and then resuspended in one-fourth volume of the above extraction buffer but without NaCl. This protein solution was loaded onto a CM-25 carboxymethyl-Sephadex column (1 mL of bed/5–10 mg of protein) equilibrated with the same buffer, and then nuclease protein was eluted in the same buffer made 0.4 M in NaCl. At this step, the protein was concentrated by precipitation (1 volume of water, 4 volumes of ethanol, 4 volumes of acetone) and the pellet collected by centrifugation and then dissolved in 1 mL of 6 M urea/30 mM sodium formate, pH 3.1. After this solution was loaded onto a Pharmacia FPLC Mono S column, protein was eluted with a gradient from 0.25 to 0.45 M NaCl. The major peak was collected, precipitated as above, dissolved in 4 M urea/10 mM Tris·HCl, pH 7.4, and then dialyzed overnight at 4 °C against 50 mM NaCl/0.5 mM PIPES buffer, pH 6.8.

Protein Analysis. Protein concentrations of nuclease fragments were determined by absorbance at 293 nm in 0.1 N NaOH by using the molar extinction coefficient of 2390 for tyrosine at this pH (Goodwin & Morton, 1946; Kuliopulos et al., 1989) and the known tyrosine content of each fragment (7 for 1–136 and 1–128; 5 for 1–112 and 1–103; no tryptophan residues). The concentration of wild-type nuclease (1–149) was determined by using the extinction coefficient at 280 nm of 0.93 (Fuchs et al., 1969). Protein purity was monitored by SDS-polyacrylamide gel electrophoresis followed by staining with Coomassie Brilliant Blue and by gel filtration chromatography and monitoring of the UV absorbance at 280 nm.

The sequence of the first four amino acid residues of fragment 1–128(wt) was determined on an Applied Biosystems Model 470A sequenator equipped with on-line PTH analysis using the regular program 03RPTH. The PTH derivatives were separated by reverse-phase HPLC over an Applied Biosystems C-18 column. After hydrolysis of fragment 1–128(wt) for 24 h at 110 °C in 6 N HCl containing 1% phenol and derivatizing the hydrolysate with phenyl isothiocyanate (Bidlingmeyer et al., 1984), amino acid analysis was performed on a Waters–Millipore Pico-Tag system calibrated with a standard mixture of amino acids. Both instruments are part of the Johns Hopkins University Protein/Peptide Facility.

Nuclease Activity Assays. Enzyme activity was measured by monitoring the increase in absorbance at 260 nm on addition of enzyme to 1 mL of a solution containing 50 μg/mL boiled salmon sperm DNA/25 mM Tris·HCl, pH 8.8/10 mM $CaCl_2$ (Cuatrecasas et al., 1967). One unit is defined as an increase of 1 OD/min. A Gilford 260 spectrophotometer with a Gilford 6051 recorder was used to determine the initial velocity of reactions carried out at room temperature. In assays of activity as a function of NaCl concentration, these same conditions were used except the $CaCl_2$ concentration was reduced to 1 mM.

Circular Dichroism. An AVIV 60DS spectrometer was used for all circular dichroism measurements. For spectra, a Hellma rectangular demountable cuvette made of Suprasil quartz with a 0.1-mm path length was used; for measurements of ellipticity at 222 nm as a function of Gdn·HCl concentration, 1 cm × 1 cm path length cuvettes with a small magnetic stir bar in the bottom for mixing were used. Spectra are the average of a series of seven scans made at 0.5-nm intervals, 1-s signal integration time, and 1.5-nm bandwidth which have been corrected relative to an appropriate base-line scan (buffer plus solutes) and then smoothed by using a third-order polynomial with ±2-point average algorithm. All measurements were made with samples held in a water-jacketed cuvette holder maintained at 20.0 ± 0.2 °C. Thymidine 5′-monophosphate (dTMP) and thymidine 3′,5′-bisphosphate (pdTp) were purchased from P-L Pharmacia Biochemicals.

Gel Filtration. A Pharmacia FPLC system equipped with a UV-1 monitor and an LKB recorder was used with a Superose-12 column (1 cm × 30 cm). The buffer (0.2 M

[1] Abbreviations: CD, circular dichroism; Gdn·HCl, guanidinium chloride; dTMP, deoxythymidine 5′-phosphate; pdTp, deoxythymidine 3′,5′-bisphosphate; Tris-HCl, tris(hydroxymethyl)aminomethane hydrochloride; PTH, phenylthiohydantoin derivative; SDS, sodium dodecyl sulfate; PIPES, piperazine-*N*,*N*′-bis(2-ethanesulfonic acid); EDTA, ethylenediaminetetraacetic acid; wt, wild type.

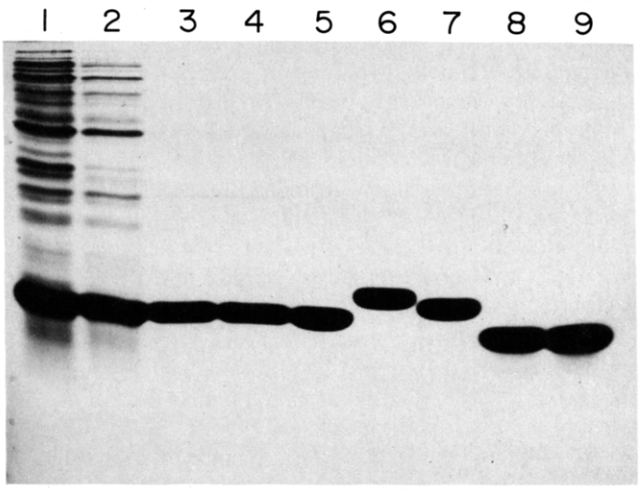

FIGURE 1: Assay of the purification and purity of nuclease fragments by electrophoresis on an SDS–18% polyacrylamide gel stained with Coomassie Brilliant Blue. Lanes: (1) whole *E. coli* cells induced for production of fragment 1–128(wt); (2) 6 M urea extract of cells; (3) pellet from second ethanol precipitation of extract; (4) fragment 1–128(wt) after first column; (5) fragment 1–128(wt) after second column; (6) wild-type nuclease (1–149); (7) fragment 1–136(wt); (8) fragment 1–112(wt); (9) fragment 1–103.

NaCl/25 mM NaH_2PO_4, pH 7.0/0.02% NaN_3, with varying concentrations of Gdn·HCl) was pumped at a rate of 0.5 mL/min, and the recorder was set at 0.5 cm/min. Reproducibility of elution volumes was typically ±0.02 mL or better. All column runs were made at room temperature (21–23 °C).

Results

Fragment Purification. In order to produce large quantities of fragments of staphylococcal nuclease, plasmid pL9 was modified by the introduction of single TAA stop codons at positions 104, 113, 129, and 137. When whole-cell lysates of bacteria induced for production of the 1–149, 1–136, 1–128, 1–112, and 1–103 protein fragments were run on 18% polyacrylamide gels containing SDS, the level of accumulation was in each case estimated to be approximately 25–50% of the Coomassie-stained material (see Figure 1). Since examination of induced cells under a phase contrast microscope revealed an increase in refractility, we conclude that the nuclease fragments are accumulated in inclusion bodies and thereby protected from proteolysis.

Initial attempts at isolation of nuclease fragments after mechanical disruption of induced cells, however, indicated that proteolysis during purification could be a serious problem. Therefore, an isolation strategy was developed that employed aqueous solutions of 6 M urea as the solvent in every step until the fragments were pure, at which point the urea was removed by dialysis. As evident in Figure 1, levels of purity greater than 98–99% were achieved. Incubation of samples at room temperature for 24–48 h revealed very little or no detectable proteolysis. Fragment purity was also monitored by analytical gel filtration on a Pharmacia Superose 12 column. Fragment 1–128(wt) was submitted to amino acid analysis and sequencing of its first four amino acid residues. Greater than 97% of peptide chains began with the predicted sequence Ala-Thr-Ser-Thr. In addition, 3.02 serine residues were found per molecule, in excellent agreement with the predicted number of three. Since serine is residue number 128, these results indicate that both carboxy and amino termini are intact in the large majority of polypeptide chains for this nuclease fragment. Similar results with fragment 9–103 also provided evidence for length homogeneity for a peptide only 95 amino acids long.

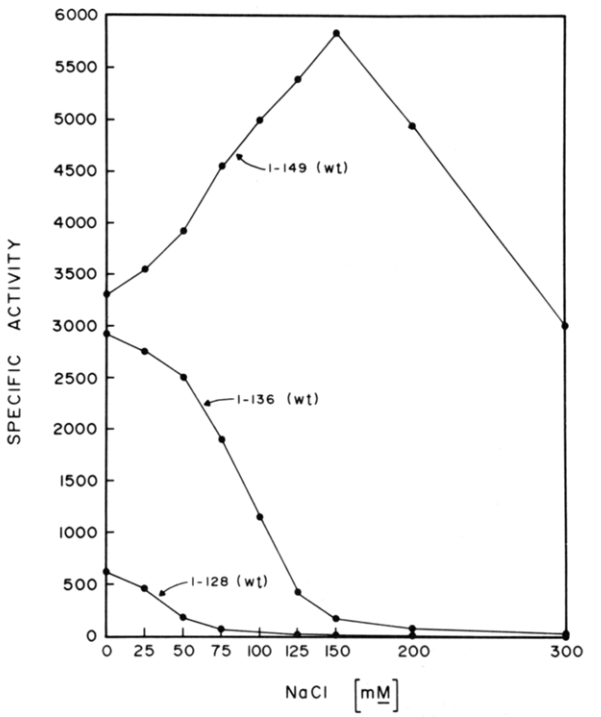

FIGURE 2: Plot of hydrolytic activity of single-stranded DNA versus sodium chloride concentration for wild-type staphylococcal nuclease and two large fragments.

Catalytic Activity. The specific activity for hydrolysis of single-stranded DNA by wild-type nuclease and the four nonsense fragments was quantitated according to the spectrophotometric assay of Cuatrecasas et al. (1967). This assay, which is based on the increase in absorbance of DNA on hydrolysis, gives some day-to-day variability in the absolute values of activity; for wild-type enzyme, i.e., 1–149(wt), specific activity varied from 1800 to 3300 units/mg. Activity values relative to wild-type were as follows: for 1–136(wt), 0.9–1.1; for 1–128(wt), 0.04–0.08; for 1–112(wt), 0.0001; for 1–103(wt), 0.001.

The observations that fragment 1–136(wt) had the same catalytic activity as full-length nuclease (1–149) and that fragment 1–128(wt) had 4–8% were quite surprising in view of evidence presented below that both fragments have very large equilibrium constants for the reversible denaturation reaction (K_d). Certainly binding of Ca^{2+} and DNA should stabilize the folded form of these fragments. However, if the catalytic activity of the fragment–Ca^{2+}–DNA complexes were the same as for the wild-type nuclease (1–149) complex, then the effect of the large K_d's should be seen in proportionally large increases in the K_m for substrates (see equations below for estimating K_d from ligand titration curves). Since the K_m for DNA is 5 μg/mL for wild-type nuclease (1–149), high levels of activity are not expected for the conditions of assay.

In view of the pronounced cationic character of staphylococcal nuclease (pI = 10.2), one explanation for this discrepancy was that the unfolded forms of the fragment nucleases bind to DNA nonspecifically through electrostatic interactions in the very low ionic strength conditions of the assay, effectively increasing the local concentration of substrate. To test this possibility, enzyme activity was measured as a function of NaCl concentration. As is evident in Figure 2, wild-type nuclease (1–149) is first stimulated and then slightly inhibited by NaCl, having the same activity at 0 M as at 0.3 M. However, both fragment nucleases are dramatically inhibited with increasing concentrations of NaCl; at 0.3 M NaCl, only 0.4% (1–136) and 0.03% (1–128) of the

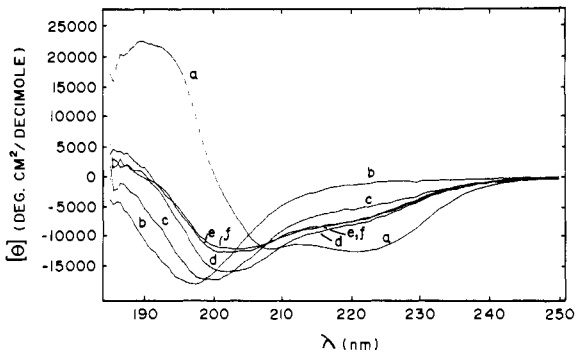

FIGURE 3: CD spectra of wild-type staphylococcal nuclease polypeptide chains. Protein concentration is 1 mg/mL in 50 mM NaCl/1 mM NaH_2PO_4, pH 6.8. (a) 1–149; (b) limit trypsin digest of 1–149; (c) 1–103; (d) 1–112; (e) 1–136; (f) 1–128.

activity at 0 M NaCl remain. Increasing the concentration of substrate DNA from 50 to 100 and 200 μg/mL in the presence of 150 mM NaCl raised the specific activity of 1–136(wt) by approximately 2- and 4-fold (data not shown). This observation supports the conclusion that the primary effect of elevated salt concentrations is to increase the K_m for DNA, presumably by decreasing nonspecific binding mediated by electrostatic interactions.

Circular Dichroism Spectra. One of the most sensitive physical methods for detecting structure in polypeptide chains is circular dichroism spectroscopy at wavelengths near the absorption band for amide bonds. Secondary structure, particularly α-helices and to a lesser extent β-sheets, is the primary determinant of the spectrum in this region. Figure 3 shows the spectrum of the native state of wild-type staphylococcal nuclease (1–149) and also the spectrum of a limit tryptic digest of wild-type nuclease, a reasonable approximation to the random coil spectrum. As is apparent from this figure, the shortest nonsense fragment (1–103) has a spectrum most similar to that of the tryptic peptides, the longest fragments (1–128, 1–136) have spectra least similar to that of the tryptic peptides, and the intermediate length fragment (1–112) is intermediate between these extremes.

All four fragments show clear evidence of some amount of residual structure. First of all, the minimum in the spectra is shifted to longer wavelengths. Second, the region between 210 and 230 nm exhibits greater negative ellipticity than for the tryptic peptides. It is unlikely that these spectral properties result from intermolecular aggregation, since spectra obtained for 1–136(wt) and 1–128(wt) at one-tenth this concentration in a cuvette with a 10-fold greater path length were essentially identical. And as described below, gel filtration of these two fragments at concentrations considerably above the 1 mg/mL level used to obtain these spectra revealed no significant dependence of the elution volume on protein concentration.

Attempts to deconvolute the spectra of these large fragments of nuclease into fractional content of α-helix, β-strand, turn, and random coil segments using the algorithm of Chang et al. (1978) provided no useful information. One reason for this may be the discrepancy between the "random coil" reference spectrum derived from known protein structures obtained by X-ray crystallography and spectra of unstructured peptides such as the tryptic digest of staphylococcal nuclease. Indeed, there is little agreement among values of this "random coil" or "nonhelical, nonsheet, nonturn" component of the protein CD spectra estimated either from known protein structures (Yang et al., 1986; Compton & Johnson, 1986) or from homopolypeptides (Adler et al., 1973).

Estimation of the Reversible Denaturation Equilibrium Constant K_d. The presence of enzyme activity in all four of the fragment nucleases suggested that these polypeptide chains are able to fold into a native or approximately native conformation. In order to estimate the equilibrium constant for the reversible denaturation reaction, i.e.

$$K_d = f_d/f_n$$

where f_d is the fraction of molecules in the denatured state and f_n is the fraction in the native state, the circular dichroism spectrum was monitored as a function of the concentration of the two tight-binding ligands Ca^{2+} and pdTp. Since for fragments 1–136(wt) and 1–128(wt) the deleted amino acid residues are remote from the active site of this enzyme, the working assumption was that the folded form of these two fragments should bind ligands with the same affinity as wild-type nuclease (1–149).

It can be shown that

$$[N^*Ca^*pdTp]/[D + N + N^*Ca^*pdTp] = [1 + (1 + K_d)/K_a[Ca][pdTp]]^{-1}$$

where N and D are the native and denatured states, respectively, and K_a is the association constant for the complex between N and Ca^{2+} plus pdTp. When half of the total molecules exist as the N*Ca*pdTp complex, then this equation can be reduced to

$$K_d = K_a[Ca][pdTp] - 1 \cong K_a[Ca][pdTp]$$

Therefore, K_d can be estimated by setting K_a equal to 1.5×10^{-8}, the value obtained for wild-type nuclease (1–149) (Serpersu et al., 1986), and by measuring the concentrations of Ca^{2+} and pdTp required to drive the equilibrium renaturation reaction to the midpoint between D and N*Ca*pdTp.

Figure 4A shows a titration of wild-type nuclease (1–149) in 4 M urea at 10 mM $CaCl_2$ with varying amounts of pdTp. This titration gives a reasonable isosbestic point at 206 nm and an approximate midpoint at 0.6 mM pdTp. By use of the equation above, these values translate into an apparent K_d of 900. By assuming a linear dependence of log K_d with respect to urea concentration as measured by intrinsic tryptophan fluorescence (Shortle & Meeker, 1986), a value of K_d in 4 M urea is estimated to be approximately 350. Since K_a is unlikely to be as large in 4 M urea as the value measured in water, a K_d of 900 is probably an overestimate and thus agrees reasonably well with the value of 350.

In Figure 4B, a titration of fragment 1–136(wt) at 10 mM $CaCl_2$ using the weaker binding ligand dTMP is shown. The K_a for the N*Ca*dTMP complex has been determined to be 1.6×10^7 M^{-2} (Serpersu et al., 1986), and with the midpoint value of approximately 1 mM dTMP, an apparent K_d of 160 is calculated. In Figure 4C, a similar titration of fragment 1–128(wt) with 25 mM $CaCl_2$ and variable concentrations of pdTp gives a midpoint value of approximately 0.5 mM nucleotide. For this fragment, the apparent K_d is 2000. And finally, in Figure 4D, results are presented for fragment 1–136 containing two amino acid substitutions—valine 66 to leucine (V66L) and glycine 88 to valine (G88V). Titration with dTMP at 10 mM $CaCl_2$ gives a midpoint concentration of approximately 10 mM nucleotide, which corresponds to an apparent K_d of 1600.

CD Spectra of Fragments Containing Amino Acid Substitutions. As described in the introduction, the impetus behind this study of large fragments of staphylococcal nuclease was to examine the effects of several interesting amino acid substitutions on the residual structure present in these experimental models of the denatured state. Figure 5A shows the circular dichroism spectra of the fragment 1–136, with either

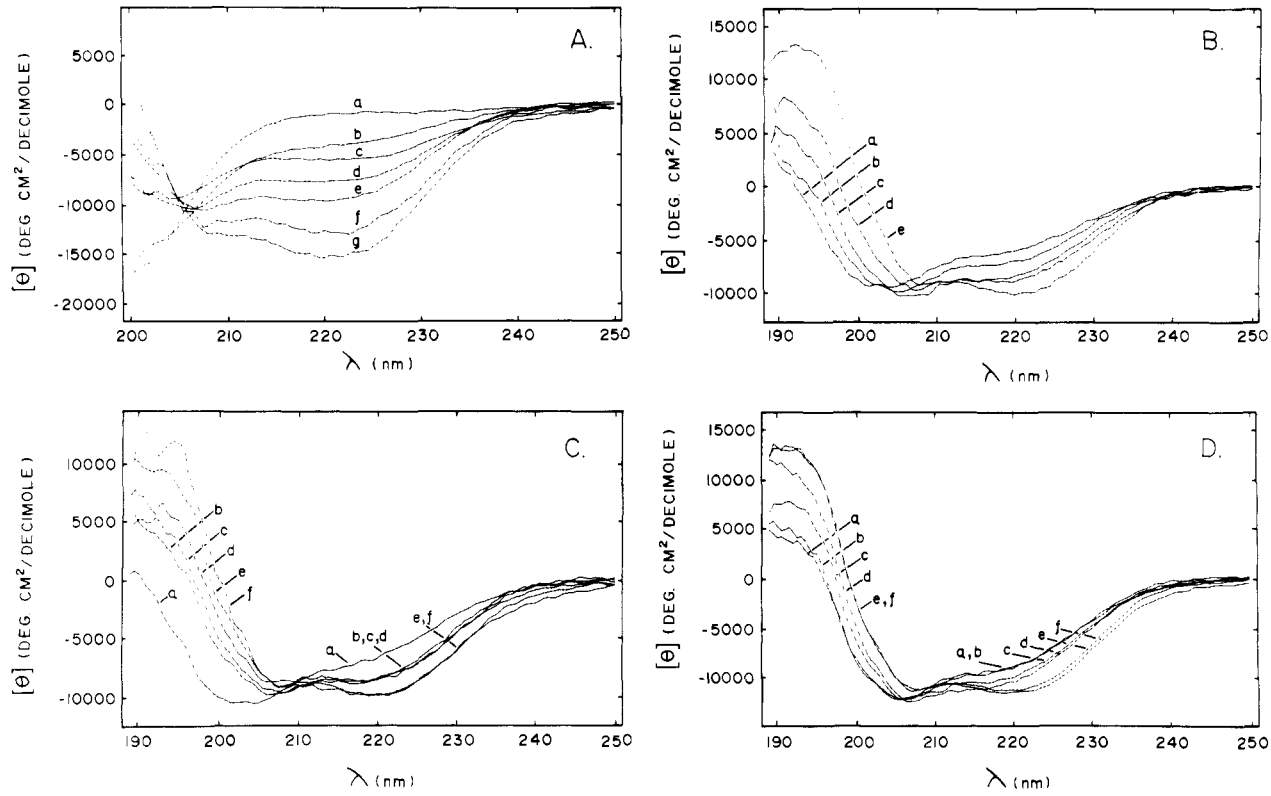

FIGURE 4: CD spectral titrations of nuclease polypeptide chains with varying concentrations of thymidine nucleotides at fixed $CaCl_2$ concentrations. Proteins concentration is 1 mg/mL in 50 mM NaCl/5 mM Tris·HCl, pH 7.4. (A) 1–149(wt) in 4 M urea and 10 mM $CaCl_2$: (a) no pdTp; (b) 0.1 mM pdTp; (c) 0.2 mM pdTp; (d) 0.4 mM pdTp; (e) 1 mM pdTp; (f) 2 mM pdTp; (g) 1 mM pdTp with no urea. (B) 1–136(wt) in 10 mM $CaCl_2$: (a) no dTMP; (b) 0.5 mM dTMP; (c) 1 mM dTMP; (d) 2 mM dTMP; (e) 2 mM pdTp. (C) 1–128(wt) in 25 mM $CaCl_2$: (a) no pdTp; (b) 0.5 mM pdTp; (c) 1 mM pdTp; (d) 2 mM pdTp; (e) 5 mM pdTp; (f) 10 mM pdTp. (D) 1–136(V66L+G88V) in 10 mM $CaCl_2$: (a) no dTMP; (b) 2 mM dTMP; (c) 5 mM dTMP; (d) 10 mM dTMP; (e) 0.5 mM pdTp; (f) 1 mM pdTp.

the wild-type sequence or with one or two amino acid substitutions. As is readily apparent, when the fragment contains substitutions A90S, A69T, or A69T+A90S, the minimum around 200 nm becomes deeper and shifts to slightly shorter wavelengths, while the ellipticity between 210 and 230 nm is less negative. Thus, for these three mutant forms (which are grouped into a class termed class II on the basis of their altered response to thermal and solvent denaturation), there is unequivocal evidence for loss of some of the structure present in the wild-type fragment.

On the other hand, when the fragment contains substitutions V66L, G88V, or V66L+G88V, the minimum around 200 nm shifts to longer wavelengths and the ellipticity between 210 and 230 nm is more negative. For these three mutant forms (which belong to a second class, termed class I, on the basis of their behavior on thermal and solvent denaturation), it can be reasonably concluded that more structure is present relative to the wild-type fragment. From the data in Figure 4D discussed above, fragment 1–136(V66L+G88V) has a larger apparent K_d than does fragment 1–136(wt). Therefore, it seems probable that the CD spectral changes caused by these two amino acid substitutions do not arise from an increase in the fraction of molecules that are folded into a native-like state.

In Figure 5B, the CD spectra of fragments 1–128 with either the wild-type amino acid sequence or the same six different mutant sequences are shown. Except for a convergence of spectra for the A90S, A69T, and A69T+A90S mutant forms, the results are remarkably similar to those obtained with the 1–136 fragments. Consequently, the same conclusions appear to hold for both sets of fragments. This is noteworthy because of the 12-fold increase in apparent K_d for fragment 1–128(wt) relative to fragment 1–136(wt). Again, taking this fact into account, it seems probable that the residual structure in all seven polypeptide chains does not represent variations in the contribution of small amounts of folded or native-like conformations to the spectra.

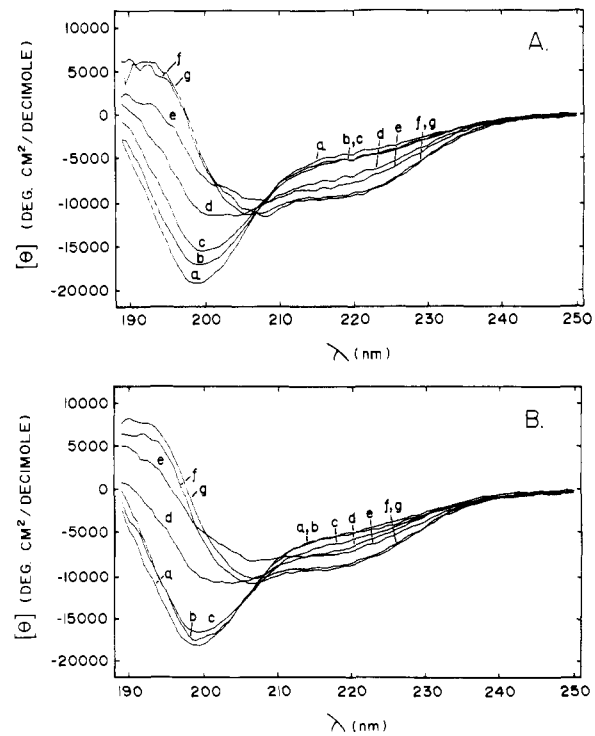

FIGURE 5: CD spectra of nuclease fragments with wild-type or mutant amino acid sequences. Protein concentration is 1 mg/mL in 50 mM NaCl/1 mM NaH_2PO_4. (A) 1–136 fragments; (B) 1–128 fragments. (a) A69T+A90S; (b) A90S; (c) A69T; (d) wild type; (e) V66L; (f) G88V; (g) V66L+G88V.

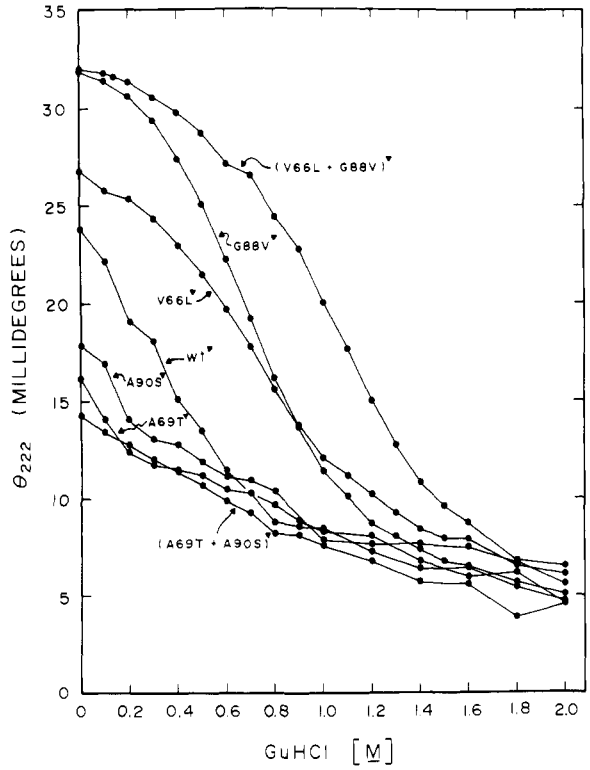

FIGURE 6: Ellipticity at 222 nm of 1–128 fragments as a function of Gdn·HCl concentration. Protein concentration is 50 μg/mL in 50 mM NaCl/10 mM NaH_2PO_4, pH 6.8.

Loss of Residual Structure on Addition of Guanidine Hydrochloride. To characterize the residual structure present in these large fragments, ellipticity at different wavelengths was monitored as a function of denaturant concentration. In Figure 6, the ellipticity at 222 nm is plotted with respect to Gdn·HCl concentration for the seven different 1–128 fragments. For the fragments containing the A69T, A90S, and A69T+A90S substitutions, the signal falls off more or less exponentially as the solution conditions become more denaturing. However, a very different result is seen for the fragments containing the V66L, G88V, and V66L+G88V substitutions. Instead of decaying exponentially, the ellipticity at 222 nm gives rise to a distinct sigmoidal curve, with V66L and G88V having the same apparent midpoint (0.7 M) but the double mutant having a midpoint shifted to 1.1 M Gdn·HCl. Although the curve for 1–128(wt) could be interpreted as approximately exponential, it can also be viewed as a sigmoidal curve with the same slope but truncated for the plateau at low denaturant concentrations. Seen in this way, its apparent midpoint is 0.3 M Gdn·HCl.

This basic experiment has been repeated numerous times using the 1–136 fragments instead of the 1–128 fragments, urea instead of Gdn·HCl, 215 or 230 nm instead of 222 nm, 0, 10, or 30 °C instead of 20 °C, and a few other amino acid substitutions (data not shown). In all instances, V66L, G88V, V66L+G88V, and other mutants of this class generate a sigmoidal curve. At 0 and 10 °C the curves for V66L, G88V, and V66L+G88V shift to lower denaturant concentrations, whereas at 30 °C, there is a small shift to higher denaturant concentrations. When the V66L+G88V double substitution is recombined into either the 1–112 or 1–103 fragments, sigmoidal curves with essentially the same midpoint value of 1.0–1.1 M Gdn·HCl are obtained (unpublished results).

Gel Filtration Analysis. To obtain an independent measure of the amount of structure present in the 1–128 fragments and to follow their response to changing denaturant concentrations,

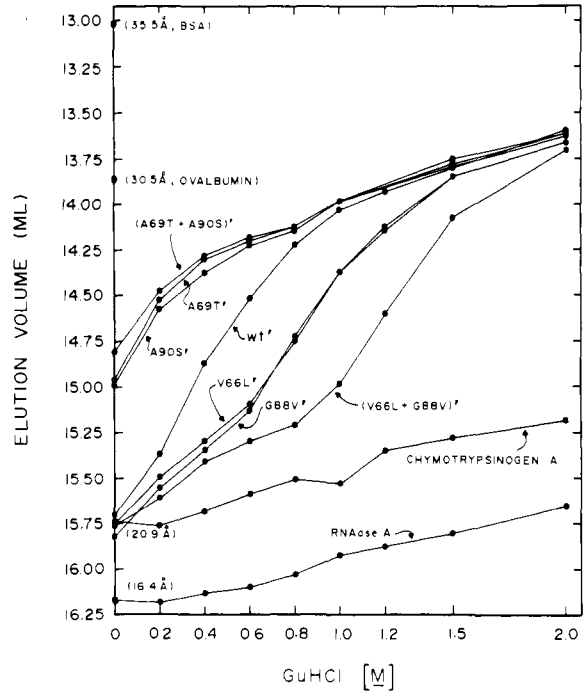

FIGURE 7: Elution volume on high-performance gel filtration analysis of 1–128 fragments as a function of Gdn·HCl concentration.

a high-performance gel filtration system was used. Slight trailing of the lagging edge of eluting peaks of fragments containing the A69T, A90S, and A69T+A90S substitutions was minimized by raising the salt concentration in the buffer to 0.2 M NaCl. Although intermolecular aggregation was not definitively ruled out for all fragments, the elution volumes of fragments 1–136(wt) and 1–128(wt) were found to be essentially independent of protein concentration over a 25-fold range (100 μL loaded at 0.2, 1.2, and 5 mg/mL). In no instance was the leading edge smeared or was any UV-absorbing material eluted either at the void volume or in a detectable plateau or peak before the main peak.

In Figure 7, elution volumes are plotted as a function of Gdn·HCl concentration for the seven 1–128 fragments, with ribonuclease A and chymotrypsinogen A serving as standards that do not undergo appreciable denaturation below 2 M Gdn·HCl (Pace, 1975). (The same slight decrease in elution volume with increasing Gdn·HCl seen for chymotrypsinogen A and ribonuclease A was also found for the fully included small molecule cytidine and may be a consequence of changes in hydration of the gel matrix.) In the absence of denaturant, fragments containing the A69T, A90S, and A69T+A90S substitutions elute considerably before fragment 1–128(wt), indicating they have larger hydrodynamic radii. Conversely, although the differences are small, fragments with the V66L, G88V, and V66L+G88V substitutions consistently exhibit greater elution volumes. Perhaps most surprising of all is the observation that, in the absence of denaturant, the elution volume of fragment 1–128(wt) is the same as that of wild-type nuclease (1–149).

As the concentration of Gdn·HCl is increased, not surprisingly, all of the fragments appear to increase in hydrodynamic radius, and at 2 M Gdn·HCl almost all of the differences present at 0 M Gdn·HCl have been erased. Yet at intermediate denaturant concentrations, the different amino acid substitutions cause rather different responses to the changing solvent conditions. The A69T, A90S, and A69T+A90S mutant forms, which initially have larger elution volumes, increase markedly in size from 0 to 0.4 M Gdn·HCl and

then relatively little at still higher concentrations. The curves for the V66L and G88V mutant forms are almost superimposable, with a gradual increase in elution volume from 0 to 0.6 M denaturant, followed by a more marked increase from 0.6 to 1.2 M, and then little change at still higher concentrations. Fragment 1–128(V66L+G88V) exhibits an even more obvious sigmoidal curve, with a midpoint around 1.2 M Gdn·HCl. If the curves for wild-type, V66L, and G88V fragments are interpreted as being sigmoidal and of essentially the same slope as that of the V66L+G88V form, then their approximate midpoints are 0.4–0.5, 0.8, and 0.8 M, respectively.

Discussion

The reversible denaturation reaction for a number of small, single-domain proteins can be fairly well approximated by a simple unimolecular interconversion between two alternative states of the polypeptide chain—the native state (N) and the denatured state (D). Although a great deal is known about the structure and dynamics of the N state for many proteins, relatively little can be said about the properties of the D state. This lack of knowledge is due in no small measure to difficulties in physically characterizing what is not a single structure but, in all likelihood, a large distribution of related structures. Furthermore, as emphasized by Lumry et al. (1966), the properties of this distribution are expected to change significantly as the conditions of solution are changed. In order to study the D state of a naturally occurring protein, which almost by definition is very unstable under physiological conditions, it is necessary to stabilize this state by working at nonphysiological conditions, such as high concentrations of denaturant, extremes of pH, or very high temperatures. And usually, under such conditions, the D state is found to contain very little or no structure [reviewed by Tanford (1969, 1971)].

An alternative approach that would permit characterization of the denatured state is to modify the chemical structure of the protein instead of the conditions of solution. One modification that arguably would result in the smallest overall perturbation of interactions that determine the structure and dynamics of the D state is the deletion of amino acids from either the carboxy-terminal or the amino-terminal end of the polypeptide chain. This approach seemed especially attractive with staphylococcal nuclease because, for this protein, both ends of the chain run along the surface of the N state for a considerable distance before entering the interior. Therefore, while important intramolecular interactions in the N state might be lost on shortening the chain, the interactions lost in the D state would be confined to residues at one end of the chain, residues that would not be expected to occupy central or buried positions. The ideal outcome would be one in which the free energy of the N state is raised by many kilocalories per mole, but the free energy of the D state would be changed very little.

Fragments 1–136 and 1–128 of staphylococcal nuclease both meet several criteria for a reasonable model of the denatured state. First of all, they contain most of the amino acid sequence of the protein. Since the last eight amino acids of wild-type nuclease (1–149) are not visible in the X-ray diffraction map (Arnone et al., 1971) and have been shown not to play a role in determining structural stability (Anfinsen et al., 1971), fragment 1–136 has lost only five important residues, leaving 96% of the chain intact. Similarly, fragment 1–128 has lost 13 important residues, leaving 91% of the chain. Second, both fragments are able to fold into a native-like state as evidenced by their high catalytic activity. Third, titration with the tight-binding ligands Ca^{2+} and either dTMP or pdTp generates a series of CD spectra that each exhibit a rough isosbestic point, lending slight support to an approximate two-state reaction between unliganded and liganded fragments. With the assumption that the affinity of the native-like states for Ca^{2+} and thymidine nucleotide is the same as for the N state of wild-type nuclease (1–149), apparent equilibrium constants can be calculated, 160 for fragment 1–136(wt) and 2000 for fragment 1–128(wt).

Both of these large fragments of staphylococcal nuclease show clear evidence of nonrandom structure under physiological conditions of solution. Their CD spectra in the 190–250-nm region are independent of protein concentration, are very similar to each other, and differ from the spectra of a set of tryptic peptides in having a minimum shifted to longer wavelengths and greater negative ellipticity between 210 and 230 nm. More striking is their small hydrodynamic radius. For fragment 1–136(wt), a value of 22 Å was obtained by gel filtration, whereas a value of 21 Å was obtained for both fragment 1–128(wt) and wild-type nuclease (1–149). These small increases in size suggest that, if these fragments are reasonable models, the denatured state of wild-type nuclease (1–149) under physiological conditions might not be larger than 24 Å in hydrodynamic radius, an approximate 15% increase in radius or 50% increase in the volume in which the chain is distributed. Clearly, such a compact configuration argues for the presence of significant nonrandomness in the statistical structure of the denatured state, since theoretical estimates of the radius of gyration for the random coil state of a polypeptide chain of this length fall in the range of 40–50 Å (Miller & Goebel, 1968).

When the amino acid sequence of these fragments was altered by substituting residues that from previous studies have been hypothesized to have significant effects on the properties of the denatured state, marked changes in the CD spectra and gel filtration behavior were found. In full-length nuclease (1–149), the three substitutions A69T, A90S, and A69T+A90S (i) increase the rate of change of free energy for the reversible denaturation reaction with respect to changes in denaturant concentration $d\Delta G/dC_{den}$ (Shortle & Meeker, 1986) and (ii) increase both the van't Hoff enthalpy change ΔH_{vH} and change in specific heat capacity ΔC_p (Shortle et al., 1988). From these two observations the inference was drawn that the denatured state containing these mutations was less structured, exposing more hydrophobic surface and total surface area to solvent. This inference is very strongly supported by the large increase in hydrodynamic radius determined by gel filtration of the 1–128 fragments. In addition, the rank order of $d\Delta G/d$[Gdn·HCl] is the same as the order of hydrodynamic radius: A90S < A69T < A69T+A90S.

The three substitutions V66L, G88V, and V66L+G88V have precisely the opposite effects on the denaturation behavior of nuclease (1–149). The rate of change of free energy with either urea or Gdn·HCl concentration is reduced relative to the wild-type value, as are the ΔH_{vH} and apparent ΔC_p (Shortle & Meeker, 1986; Shortle et al., 1988). And the inference that nuclease with these mutations has a more compact denatured state with less hydrophobic surface area and less total surface area is supported by the results of gel filtration. Although the differences in hydrodynamic radius are very small in the absence of denaturant, they become much larger at intermediate concentrations of denaturant. And again, the rank orders of $d\Delta G/d$[Gdn·HCl] and the hydrodynamic radius at low denaturant concentration are the same: V66L > G88V > V66L+G88V.

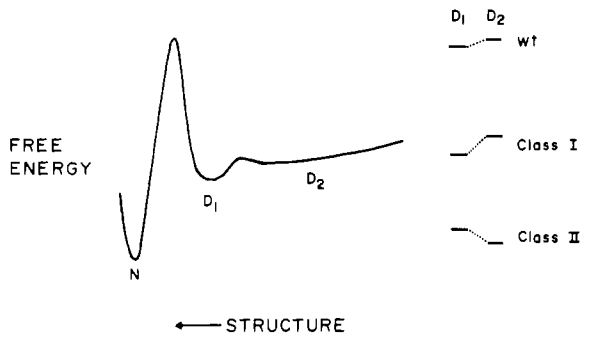

FIGURE 8: Hypothetical free energy diagram for the native state (N) and two denatured states (D1, D2) of wild-type staphylococcal nuclease (1–149) under physiological conditions of solution. Effects of class I and class II mutations on the relative stabilities of the D1 and D2 states are also shown.

The most intriguing result from these studies is the sigmoidal curves obtained when either ellipticity at 222 nm or elution volume is plotted as a function of Gdn·HCl concentration for the 1–128 fragments with the V66L, G88V, and V66L+G88V substitutions, and perhaps wild type as well. Such curves are reminiscent of conventional protein denaturation curves and suggest that a cooperative transition is occurring, one involving a significant change in free energy and the exposure of a considerable amount of new solvent-accessible surface area (Tanford, 1964; Schellman, 1978). Since the apparent midpoints for these four proteins are very similar for both the CD and the gel filtration curves, it seems likely that these two probes of structure are detecting the same transition.

Therefore, we conclude that the simplest explanation for these findings is that two alternative forms of the denatured state exist: D1, which is compact (though not as compact as the N state) and has some structure detectable by circular dichroism, and D2, which has a much larger hydrodynamic radius and shows a CD spectrum that is similar to that of a collection of random peptides. For wild-type nucleas, D1 appears to be only marginally more stable than D2 in the absence of denaturants. The effects of the A69T, A90S, and A69T+A90S substitutions on the solvent and thermal denaturation reactions, previously explained as resulting from a less structured, more solvent exposed D state, can now be explained by hypothesizing that they either stabilize D2 or destabilize D1. Likewise, the more compact, less solvent exposed D state invoked to explain the effects of the V66L, G88V, and V66L+G88V substitutions may represent a stabilization of D1 or a destabilization of D2. Rough estimates of the free energy change for the D1 to D2 reaction in the absence of denaturants can be obtained by the linear extrapolation method (Pace, 1975) and are (in kcal/mol) +0.7 for wild type, +2.2 for G88V, +2.3 for V66L, and +2.8 for V66L+G88V. These relative changes in free energy are shown diagrammatically in Figure 8. Clearly the cooperative nature of the D1 to D2 transition is evidence for a free energy barrier between these two hypothetical distributions of denatured states and thus evidence for their being resolvable distributions. These conclusions imply that the two-state approximation, as proposed by Lumry et al. (1966), does not adequately describe the equilibrium denaturation behavior of staphylococcal nuclease under some situations.

Because the concentration of the D1 state for both wild type and the three class II mutations would be expected to be very low in the range of Gdn·HCl concentration at which the full-length proteins undergo denaturation, conventional denaturation studies should only detect the N to D2 transition. However, the situation is more complex for the class I mutants. If the D1 state is present at the lower range of Gdn·HCl concentrations, then several different equilibria involving N, D1, and D2 would change as the Gdn·HCl concentration is increased, potentially giving rise to multiphasic denaturation curves (if the spectroscopic probe can detect differences between the three species) or nonsuperimposable denaturation curves obtained with different structural probes. In accordance with these expectations, full-length wild type and class II mutant (I18M+A90S) give the same monophasic sigmoidal Gdn·HCl denaturation curve by intrinsic tryptophan fluorescence and circular dichroism (Shortle & Meeker, 1986) and by intrinsic tyrosine fluorescence (unpublished data). However, the most pronounced class I mutant (V66L+G79S+G88V) gives a much broader transition when CD is monitored as opposed to intrinsic tryptophan fluorescence (Shortle & Meeker, 1986), with intrinsic tyrosine fluorescence giving a curve intermediate between these two (unpublished data). To date, these nonsuperimposable denaturation curves are the only evidence for the existence of the D1 state in full-length forms of staphylococcal nuclease.

Three points in the data argue that the hypothetical D1 state is not an exact subset of native structure. Most convincing is the fact that the stability of D1 responds differently to amino acid substitutions than does the stability of N. For D1, the order of stability is V66L+G88V > G88V > V66L > wild type, whereas for N, the order is exactly the reverse: wild type > V66L > G88V > V66L+G88V (Shortle & Meeker, 1986). This finding raises the possibility that part of the mechanism by which these amino acid substitutions result in a full-length protein of lower stability is through their stabilization of the D1 state relative to the N state. Second, although the removal of eight additional amino acid residues from 1–136(wt) to make the 1–128(wt) fragment lowers the stability of N by approximately 1.5 kcal/mol, it has no detectable effect on the stability of D1 as assessed by the slopes and midpoints of ellipticity at 222 nm versus Gdn·HCl concentration curves. And finally, fragment 1–136(V66L+G88V) in the absence of denaturant may be assumed to represent a pure D1 state. The CD spectrum for this chain, which is 96% of full length, is markedly different from the N state of wild-type nuclease (1–149).

Attempts to define the amount and type of structure present in the D1 state are currently under way. This task should be simplified by the finding that fragment 9–103(V66L+G88V) displays essentially the same cooperative structure breakdown in Gdn·HCl as larger fragments with these two substitutions. Since this segment of the polypeptide chain contains virtually all of the hydrophobic core centered in the five-strand β-barrel structure and since D1 appears to be stabilized by amino acid substitutions that increase hydrophobicity and to be destabilized by substitutions that replace hydrophobic amino acids with polar ones, we speculate that D1 represents a micelle-like state held together primarily by hydrophobic interactions. On considering the approximate cylindrical shape of the five β-strands and two α-helices present in the native state between residues 9 and 103, we further speculate that D1 may consist of a very small smectic liquid-crystalline structure in which the chain segments that form the strands and helices assume a more parallel alignment.

If the 1–128 fragments containing substitutions A69T, A90S, and A69T+A90S are assumed to represent a pure population of polypeptide chains in the D2 state, then it appears that this state has a small amount of residual structure that is removed gradually with increasing concentrations of denaturant. The picture of the protein-folding process that

emerges from this line of reasoning is similar to one proposed by Dill (1985), in which the formation of structure is a coupled to a collapse to a hydrophobic core. However, the data presented here suggest that the end product of such a collapse may not be the native state, but rather a compact state lacking some of the secondary structure present in the native state. Presumably this D1 state is subsequently converted into the native state in a highly cooperative transition involving formation of additional secondary structure.

The strong correlation between changes in $d\Delta G/dC_{den}$ and changes in the hydrodynamic radius on gel filtration supports the conclusion that changes in the value of $d\Delta G/dC_{den}$ for a particular protein represent changes in the additional protein surface ΔA exposed to solvent on denaturation. When $d\Delta G/dC_{den}$ increases for a mutant nuclease (1–149), and thus ΔA increases, a larger hydrodynamic radius of the mutant fragment (1–128) is observed. Likewise, when $d\Delta G/dC_{den}$ decreases, a smaller hydrodynamic radius is observed. However, this qualitative agreement is complicated by the fact that the hydrodynamic radius, and therefore presumably ΔA, changes with changing denaturant concentration. In view of this observation, the remarkable constancy of $d\Delta G/dC_{den}$ over considerable ranges of denaturant concentration for staphylococcal nuclease and other proteins (Pace, 1975; Shortle & Meeker, 1986; Shortle, Meeker, and Gerring, unpublished results) becomes an even greater puzzle. Clearly, there is much that remains to be learned about the mechanism of action of denaturants like Gdn·HCl and urea.

In summary, the data described in this report demonstrate that single amino acid substitutions can profoundly alter the residual structure present in large amino-terminal fragments of staphylococcal nuclease. If the physical properties of these large fragments are representative of the denatured state of the full-length protein under similar conditions of solution, then the conclusion seems secure that there is structure in the denatured state that can be modified by single amino acid substitutions. In view of this conclusion, discussions of the mechanism by which specific mutations alter the stability of a protein must include the real possibility that some, if not all, of the energetically important perturbations occur in the denatured state.

Acknowledgments

We thank John Gerlt for his generous gift of the pNJS expression plasmid, Murthi Shenbagamurthi for conducting the amino acid analysis and N-terminal sequencing of fragment 1–128(wt), and Al Mildvan for suggesting the Ca^{2+} and pdTp titrations of the CD spectra to determine apparent values of K_d for the nuclease fragments.

Registry No. Staphylococcal nuclease, 9013-53-0.

References

Adler, A. J., Greenfield, N. J., & Fasman, G. D. (1973) *Methods Enzymol. 27*, 675.

Anfinsen, C. B., Cuatrecasas, P., & Taniuchi, H. (1971) *Enzymes (3rd Ed.) 4*, 177–204.

Arnone, A., Bier, C. J., Cotton, F. A., Day, V. W., Hazen, E. E., Jr., Richardson, D. C., Richardson, J. S., & Yonath, A. (1971) *J. Biol. Chem. 246*, 2302–2316.

Aune, K. C., Salahuddin, A., Zarlengo, M. H., & Tanford, C. (1967) *J. Biol. Chem. 242*, 4486–4489.

Bidlingmeyer, B. A., Cohen, S. A., & Tarvin, T. L. (1984) *J. Chromatogr. 336*, 93–104.

Chang, C. T., Wu, C. C., & Yang, J. T. (1978) *Anal. Biochem. 91*, 13–31.

Compton, L. A., & Johnson, W. C., Jr. (1986) *Anal. Biochem. 155*, 155–167.

Cuatrecasas, P., Fuchs, S., & Anfinsen, C. B. (1967) *J. Biol. Chem. 242*, 1541–1547.

Dill, K. A. (1985) *Biochemistry 24*, 1501–1509.

Flory, P. J. (1953) in *Principles of Polymer Chemistry*, Chapter XII, Cornell University Press, Ithaca, NY.

Fuchs, S., Cuatrecasas, P., & Anfinsen, C. B. (1967) *J. Biol. Chem. 242*, 4768–4770.

Goodwin, T. W., & Morton, R. A. (1946) *Biochem. J. 40*, 628–632.

Hibler, D. W., Stolowich, N. J., Reynolds, M. A., Gerlt, J. A., Wilde, J. A., & Bolton, P. H. (1987) *Biochemistry 26*, 6278.

Kuliopulos, A., Mildvan, A. S., Shortle, D., & Talalay, P. (1989) *Biochemistry* (in press).

Lumry, R., Biltonen, R., & Brandts, J. F. (1966) *Biopolymers 4*, 917.

Miller, W. G., & Goebel, C. V. (1986) *Biochemistry 7*, 3925–3935.

Mott, J. E., Grant, R. A., Ho, Y.-S., & Platt, T. (1985) *Proc. Natl. Acad. Sci. U.S.A. 82*, 88–92.

Pace, C. N. (1975) *Crit. Rev. Biochem. 3*, 1–43.

Schellman, J. A. (1978) *Biopolymers 17*, 1305–1322.

Serpersu, E. H., Shortle, D., & Mildvan, A. S. (1986) *Biochemistry 25*, 68–77.

Shortle, D., & Lin, B. (1985) *Genetics 110*, 539–555.

Shortle, D., & Meeker, A. K. (1986) *Proteins: Struct., Funct., Genet. 1*, 81–89.

Shortle, D., Meeker, A. K., & Freire, E. (1988) *Biochemistry 27*, 4761–4768.

Tanford, C. (1964) *J. Am. Chem. Soc. 86*, 2050.

Tanford, C. (1968) *Adv. Protein Chem. 23*, 121–282.

Tanford, C. (1970) *Adv. Protein Chem. 24*, 1–95.

Tsong, T. Y. (1974) *J. Biol. Chem. 249*, 1988–1990.

Yang, J. T., Wu, C. C., & Martinez, H. M. (1986) *Methods Enzymol. 130*, 208–269.